

# Application of Nanoclay Materials in Asphalt Pavements

## Authors:

### **Thomas W. Johnson**

MSc Student, University of Alberta  
1-060 Markin/CNRL Natural Resources Engineering Facility  
9105 116th St.  
Edmonton, AB Canada T6G 2W2  
(e-mail) [twjohnso@ualberta.ca](mailto:twjohnso@ualberta.ca)

### **Leila Hashemian, Ph.D. (corresponding author)**

Assistant Professor, University of Alberta  
Department of Civil & Environmental Engineering  
7-255, Donadeo Innovation Centre for Engineering  
9211 116th St., University of Alberta  
Edmonton, AB, Canada T6G 1H9  
(e-mail) [hashemia@ualberta.ca](mailto:hashemia@ualberta.ca)  
780-492-8934

### **Sidharth Patra**

Summer Student Intern, University of Alberta  
(e-mail) [patra@ualberta.ca](mailto:patra@ualberta.ca)

### **Azar Shabani**

Postdoctoral Fellow, University of Alberta  
(e-mail) [azar1@ualberta.ca](mailto:azar1@ualberta.ca)

Paper prepared for presentation at the Innovations in Pavement Management, Engineering and Technologies Session of the 2019 TAC-ITS Canada Joint Conference

Halifax, NS

## **Abstract**

Heavy vehicle loads and seasonal temperature changes can influence the rheological and mechanical properties of asphalt mixtures in flexible pavements. Pavements designed and constructed for heavy-duty traffic under extreme weather conditions generally require engineered asphalt cement modification. Depending on the required type of improvement, proper modifier(s) should be introduced to improve the properties of the asphalt cement. Recently, nanomaterials with sizes of 1 to 100 nm have been introduced as potential asphalt modifiers. These particles, with their high surface area to volume ratio, possess unique bulk, surface, and colloidal properties. Based on previous studies, the addition of nanoclay, nanocarbon, and nanosilica can improve the rheological properties of asphalt cement and, consequently, also affect its mechanical properties, such as tensile strain, flexural strength, and elasticity.

Previous studies suggest that nano-clays, although not widely used as asphalt additives, has the potential to enhance the low-temperature properties and performance of asphalt cement. This research focused on the modification of the rheological properties of asphalt cement using two different nanoclays. The mechanical performance of hot mix asphalt (HMA) containing nanoclay-modified binders at different temperatures was also compared with that of unmodified asphalt mixes.

**Keywords:** nanomodified asphalt cement, nanoclay, rheology, mechanical properties.

## **INTRODUCTION AND BACKGROUND**

Low-temperature cracking (or thermal cracking) in hot mix asphalt (HMA) is a critical issue for many transportation agencies across North America. To address this type of cracking, the Strategic Highway Research Program (SHRP) in the US developed the Superpave mix design method, which provides the criteria for selection of the appropriate performance grade (PG) asphalt binder (Christensen & Ramon, 2004). To avoid thermal cracking in cold regions such as Canada, there is a tendency to use softer binders with lower PG for HMA layers; however, flexible pavements can also undergo severe rutting failure during the summer (Deepa et al, 2019).

In flexible pavements, both heavy vehicle loads and variation in seasonal temperatures can sway the temperature susceptibility characteristics (rheology) of asphalt binders. Consequently, the mechanical properties and long-term performance of asphalt mixtures will be affected (Jahromi & Khodaii, 2009). Pavements designed and constructed for heavy-duty traffic under extreme weather conditions generally require engineered asphalt cement modification. Depending on the characteristics required, proper modifier(s) should be introduced to improve such properties (Yue, et al., 2019). Recently, nanomaterials with at least one dimension between 1-100 nm have been introduced as potential asphalt modifiers. These particles, with their high surface area to volume ratio, possess unique bulk, surface, and colloidal properties. Based on previous studies, the addition of nanoclay, nanocarbon, or nanosilica can improve the rheological properties of asphalt cement and, consequently, its mechanical properties, such as tensile strain, flexural strength and elasticity (Yao, et al., 2012). This research focused on the rheological properties of asphalt cement modified using two different nanoclays, bentonite and halloysite.

Since the early 1970s, synthetic polymers [with the most common being the elastomer, styrene butadiene styrene (SBS)] have been employed to modify the performance of bituminous binders, resulting in decreased temperature susceptibility, increased cohesion and modified rheological characteristics (Ajour, 1981). However, current trends in the industry have involved investigating the application of nanotechnology for modification of HMA pavements. Though limited studies of nanotechnology application in HMA pavements have been conducted, a preliminary cost analysis revealed that nano-modification of asphalt binder is 22 – 33% cheaper than its polymer-modified equivalent (Ghile, 2006).

### **Nanotechnology**

Nano (1 billionth) is derived from a Greek word which means dwarf, is approximately 1/80000 the diameter of the human hair (Zhu et al, 2004) and is used to refer to dimensions in the range of 0.1 to 100 nm. Due to their high surface area to volume ratio and small dimensions, nanomaterials have been observed to significantly alter properties at the macro level, since quantum effects come into play. As a leading technology the world over, nanotechnology provides an opportunity to create new structures with enhanced functional properties which are more cost-effective and efficient in almost all areas of technology (Deepa et al, 2019).

### **OBJECTIVES AND SCOPE**

The objective of this paper is to investigate and compare the effects of nanoclays on asphalt rheology and HMA performance. For this purpose, asphalt samples were mixed using one of two different nanoclays – hydrophilic bentonite nanoclay and halloysite nanotubes – using a high shear mixer. Scanning electron microscopy (SEM) was used to investigate the dispersion of the nanoclay in the base asphalt after mixing. Frequency sweeps were performed between 4°C and 40°C and master curves were plotted at 20°C to evaluate complex modulus ( $G^*$ ) and phase angle ( $\delta$ ) of the modified and non-modified asphalt samples using a dynamic shear rheometer (DSR). Viscosity measurements were taken to verify and determine the

mixing and compaction temperatures of the control and nanoclay-modified asphalt mix specimens, respectively. Hamburg wheel tracker tests were conducted on hot-mix asphalt samples prepared from the normal asphalt binder, as well as the nanoclay-modified asphalt binder, to evaluate and compare the resistance of the samples to rutting and susceptibility to moisture. Indirect tensile (IDT) tests were also performed to evaluate the cracking potential of asphalt mixes at low temperatures.

## **MATERIALS**

### **Asphalt**

The asphalt binder used in this study was PG 58-31 (provided by Husky Energy), meaning it met performance criteria for a 7-day average maximum pavement temperature of 58°C and at a minimum pavement temperature of -31°C (Federal Highway Authority/National Highway Institute, 2000).

### **Halloysite Nanoclay**

For this research, halloysite nanoclay (kaolin) with a formula of  $H_4Al_2O_9Si_2 \cdot 2H_2O$ , with a molecular weight of 294.19 g/mol, and density of 2.53 g/cm<sup>3</sup>, in the form of a nanopowder was used. It has a tube-like morphology, with diameters ranging between 30-70 nm and lengths of 1-3 μm. It appears as a white to tan powder, has a pore volume of 1.26 – 1.34 mL/g, specific gravity of 2.53, and surface area of 64 m<sup>2</sup>/g (Merck KGaA/Sigma-Aldrich, 2019). Although it exhibits low electrical and thermal conductivity, it possesses strong hydrogen interactions due to its inner hydroxyl groups. The application of halloysite nanoclay as a reinforcement in nanocomposites has yielded improvements in thermal and mechanical properties, likely due to its characteristic tube-like morphology and high aspect ratio (Marini J et al, 2014).

### **Nanoclay, Hydrophilic Bentonite**

Bentonite is an absorbent aluminum phyllosilicate clay, which consists mainly of montmorillonite, a subclass of smectite. It is composed of two tetrahedral silicon oxide layers sandwiching an octahedral aluminum oxide layer, with a chemical formula of  $H_2Al_2O_6Si$  and a molecular weight of 180.1 g/mol. It exists in powder form with a particle size less than or equal to 25μm (Sigma-Aldrich, 2018). Although clay platelets have negatively charged surfaces, the replacement of aluminum atoms in the octahedral layer with other cations (sitting on top of the tetrahedral silicon layer) tends to balance the charge in the octahedral layer, which creates a charging defect. The ability of bentonite to readily trade these surface cations in exchange for hydratable, as well as organic, cations makes the normally hydrophilic montmorillonite hydrophobic (or generates organically treated clays); consequently, making it dispersible in polymer matrices (Morgan, 2007).

### **Preparing the modified asphalt sample**

Modified asphalt samples were prepared by adding the nanoclays to the base asphalt binder (PG 58-31) in the proportions shown in Table 1. To prepare the modified binder sample, 500 g of PG 58-31 asphalt binder was poured in a cylindrical tin container and heated to a temperature around 140°C on a hot plate to maintain this temperature while a high shear mixer was used (Figure 1). Using this arrangement of mixer and hot plate, the nanomaterial was added to the asphalt binder and mixed at a shear rate of 5500 – 6000 rpm for 4.5 hours.

Table 1: Amount of nanomaterial added to base asphalt binder (% by weight)

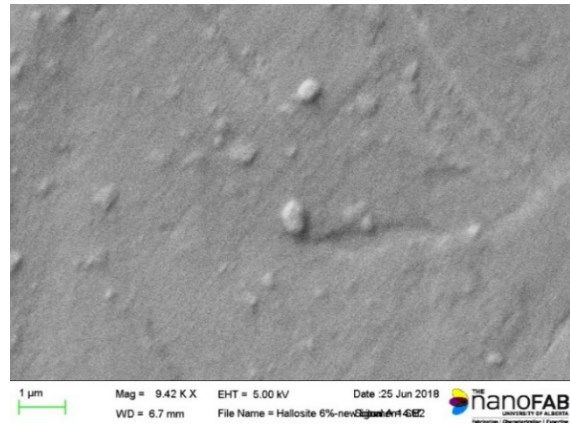
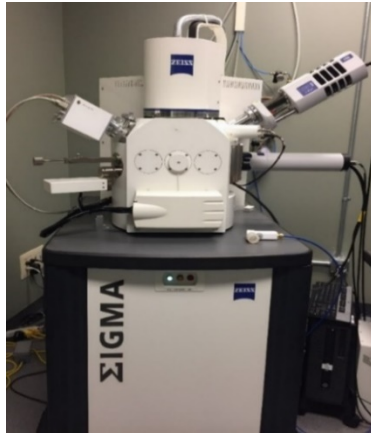
Nanomaterial	Amount added to base asphalt binder (% by weight)
Halloysite Nanoclay	3 and 6
Nanoclay, Hydrophilic Bentonite	3 and 6



Figure 1: High shear mixer with a hot plate beneath: setup for preparing binders modified with nanoclay.

### Qualitative Evaluation of Modified Asphalt Binder Samples

A Zeiss Sigma Field Emission Scanning Electron Microscope (FESEM) was used to evaluate the dispersion of nanoclay in the asphalt binder qualitatively. Asphalt samples were first sputter-coated with gold using Denton Vacuum gold coating equipment to improve their conductivity. This coating increases the number of secondary electrons that can be detected from the surface of the specimen in the SEM. For SEM, the sputtered films typically have a thickness range of 2 to 20 nm (Leica Microsystems GmbH [DE], 2018). Figure 2 shows the SEM equipment (2-a) and also an example of the dispersion of the nanoclay in the binder. As Figure 2-b shows, the dispersion of nanoclay samples in the binder seems to be consistent after 4.5 hours of mixing at a rate of 5500-6000 rpm.



(a)

(b)

Figure 2: (a) SEM equipment and (b) Image of modified binder using 6% by weight halloysite clay

### RHEOLOGY TESTS ON THE MODIFIED ASPHALT BINDER SAMPLES

To investigate the performance of modified binders at different temperatures and loading frequencies, rheological tests were performed. About 20 to 30 g of the prepared sample was heated in an oven in a small aluminum tray at 140°C. When the sample was sufficiently fluid, it was poured into an 8-mm diameter silicone mold (Figure 3-a). Rheological measurements were carried out using a Smartpave 102 Dynamic Shear Rheometer (DSR) from Anton Paar (Figure 3-b). Using an 8-mm diameter parallel plate, a gap of 2 mm and an angular frequency range of 0.3 to 300 rad/s, frequency sweep tests were performed on the samples through loop temperatures of 40°C, 30°C, 20°C, 10°C and 4°C. The parameters calculated were the complex modulus ( $G^*$ ), phase angle ( $\delta$ ) and rutting parameter ( $G^*/\sin(\delta)$ ).

A minimum of four tests were conducted for each of the modified samples, as well as the base asphalt binder. The average of the results for each sample was used to determine the effect of modification on the asphalt binder. Data measurements were then taken for the target temperature of 20°C and a broader frequency range using the time-temperature superposition principle and the Williams-Landel-Ferry (WLF) equation. This was performed using Rheoplus software (Anton Paar).



(a)



(b)

Figure 3: DSR test (a) sample, (b) testing equipment

The base asphalt PG 58-31 was modified with halloysite nanoclay in two different proportions (3% and 6% by weight). Complex modulus ( $G^*$ ) versus angular frequency curves, as well as phase angle ( $\delta$ ) versus angular frequency curves, at the target temperature of 20°C were analysed for the base asphalt specimens, as well as those of the modified asphalt, and their values were compared. An increase in the value of complex modulus leads to improvement in the rutting parameter ( $G^*/\sin(\delta)$ ).  $G^*/\sin(\delta)$  is a quantity to determine the susceptibility of HMA (prepared with a specified performance grade asphalt binder) to rutting (Table 2) (Federal Highway Authority/National Highway Institute, 2000).

Table 2: Performance Graded Asphalt Binder DSR specifications (as summarized from Superpave Fundamentals (Federal Highway Authority/National Highway Institute, 2000))

Material	Quantity	Specification	HMA Distress of Concern
Unaged binder	$G^*/\sin(\delta)$	$\geq 1.0$ kPa (0.145 psi)	Rutting
RTFO residue	$G^*/\sin(\delta)$	$\geq 2.2$ kPa (0.319 psi)	Rutting
PAV Residue	$G^* \cdot \sin(\delta)$	$\geq 5,000$ kPa (725 psi)	Fatigue Cracking

### Samples Modified with Halloysite Nanoclay

Figure 4-a shows that asphalt samples modified using halloysite showed an improvement in the complex modulus (increase) at low frequencies, with little or no change at high frequencies. There was a greater increase in the  $G^*$  value for the binder containing 6% by weight halloysite than for the binder containing 3% halloysite. Rutting parameter ( $G^*/\sin(\delta)$ ) versus angular frequency was also plotted, and the results compared (Figure 4-b). As there was not a significant reduction in phase angle due to halloysite modification, there was an improvement in the rutting parameter similar to  $G^*$  (Figure 5).

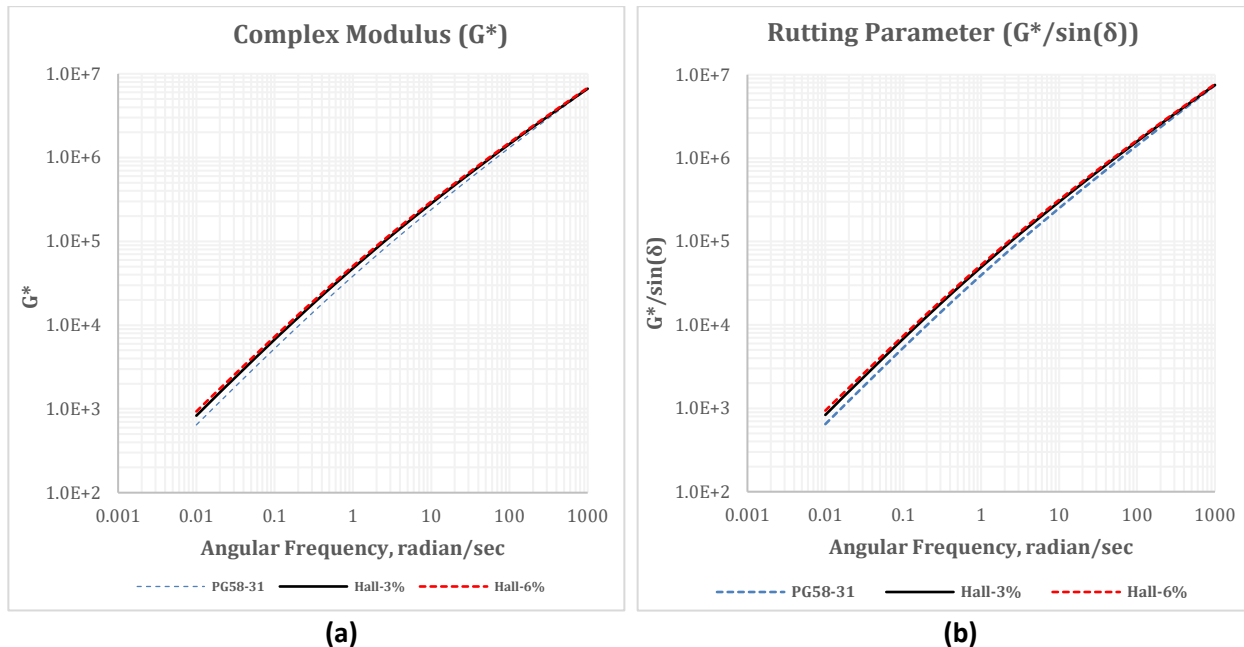


Figure 4: Halloysite modified binder at 20°C – (a) Complex Modulus and (b) Rutting Parameter

## Samples Modified with Bentonite Nanoclay

Like halloysite nanoclay, the asphalt samples modified using bentonite nanoclay showed an improvement (increase) in the complex modulus at low frequencies with little or no change at high frequencies (Figure 5-a). Using 6% of the bentonite nanoclay by weight in the binder increased the  $G^*$  value compared to the mixture containing 3% by weight. The rutting parameter ( $G^*/\sin(\delta)$ ) was also plotted with against angular frequency and the results were compared for the different mixtures (3%, 6% and control) (Figure 5-b). As Figure 5-b shows, the addition of more halloysite nanoclay led to a higher rutting resistance.

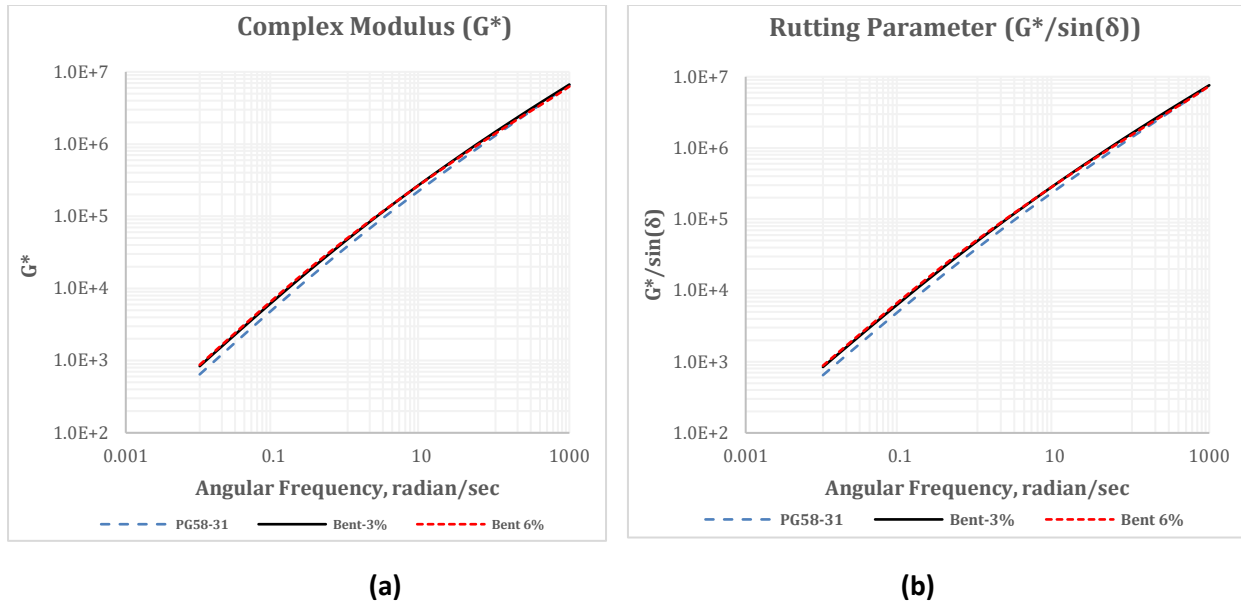


Figure 5: Bentonite modified binder at 20°C – (a)Complex Modulus and (b) Rutting Parameter

## PERFORMANCE TESTS

### HMA Mix Design

The HMA mix design used for this research was based on the Superpave mix design procedure for a 10 mm – High Traffic (HT) asphalt layer. The grain size distribution and asphalt mix properties of the aggregates summarized in Tables 3 and 4 below were provided by Lafarge, Canada in consonance with Table 3.53.2.2A of the Standard Specification for Highway Construction (Alberta Transportation, 2010). The same mix design was used for preparing all modified and unmodified asphalt samples. Figure 6 shows the aggregate gradation curve with respect to the upper and lower limits.

Table 3: Aggregate grain size distribution

Sieve Size (mm)	% Passing
12.5	100
10	98.3
8	88.5
6.3	75.4
5	64.8
2.5	49.0
1.25	39.5
0.63	32.7
0.315	20.2
0.16	10.3
0.08	5.1

Table 4: Asphalt mix properties

Properties	Actual	Specifications
Number of gyrations	100	100
A.C. % of Total Mix	5.5	-
G <sub>mm</sub> (kg/m <sup>3</sup> )	2431	-
G <sub>mb</sub> (kg/m <sup>3</sup> )	2337	-
Air voids (%)	3.9	3.6 – 4.4
VMA (%)	14.9	13 min
VFA (%)	73.8	70 – 80
% G <sub>mm</sub> @ N <sub>max</sub>	96.8	98.0 max
Dust/AC	1.0	-

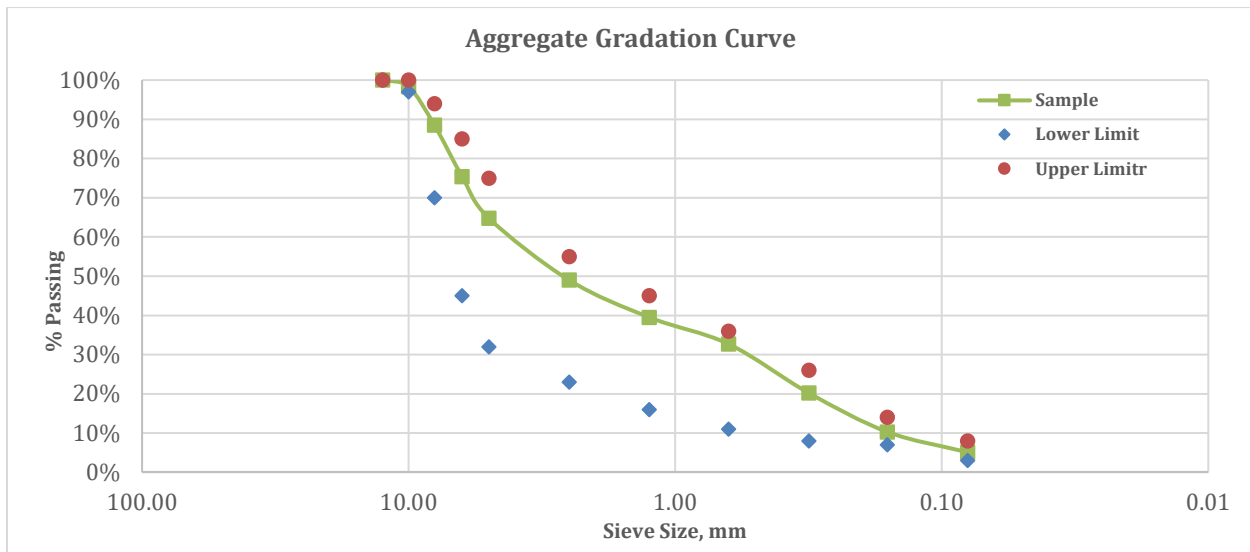


Figure 6: Aggregate Gradation Curve

### Mixing and Compaction Temperatures

To select the appropriate mixing and compaction temperatures for each modified and unmodified asphalt sample, a Fungilab EVO Expert Rotational Viscometer (RV) was used. In this measurement, the torque required to maintain a cylindrical spindle submerged in an asphalt binder sample at a constant rotational speed of 20 revolutions per minute (RPM) at constant temperature is determined. This torque is converted to viscosity and displayed automatically by the equipment.

Figure 7 shows the viscosity curves for the neat asphalt binder, along with the four nanomodified binders. Based on these results, the mixing and compaction temperatures used for sample preparation were:

- PG 58-31 (Mixing = 145°C; Compaction = 135°C)
- 3% Halloysite-modified PG 58-31 (Mixing = 150°C; Compaction = 140°C)
- 6% Halloysite-modified PG 58-31 (Mixing = 155°C; Compaction = 144°C)
- 3% Bentonite-modified PG 58-31 (Mixing = 150°C; Compaction = 140°C)

- 6% Bentonite-modified PG 58-31 (Mixing = 155°C; Compaction = 144°C)

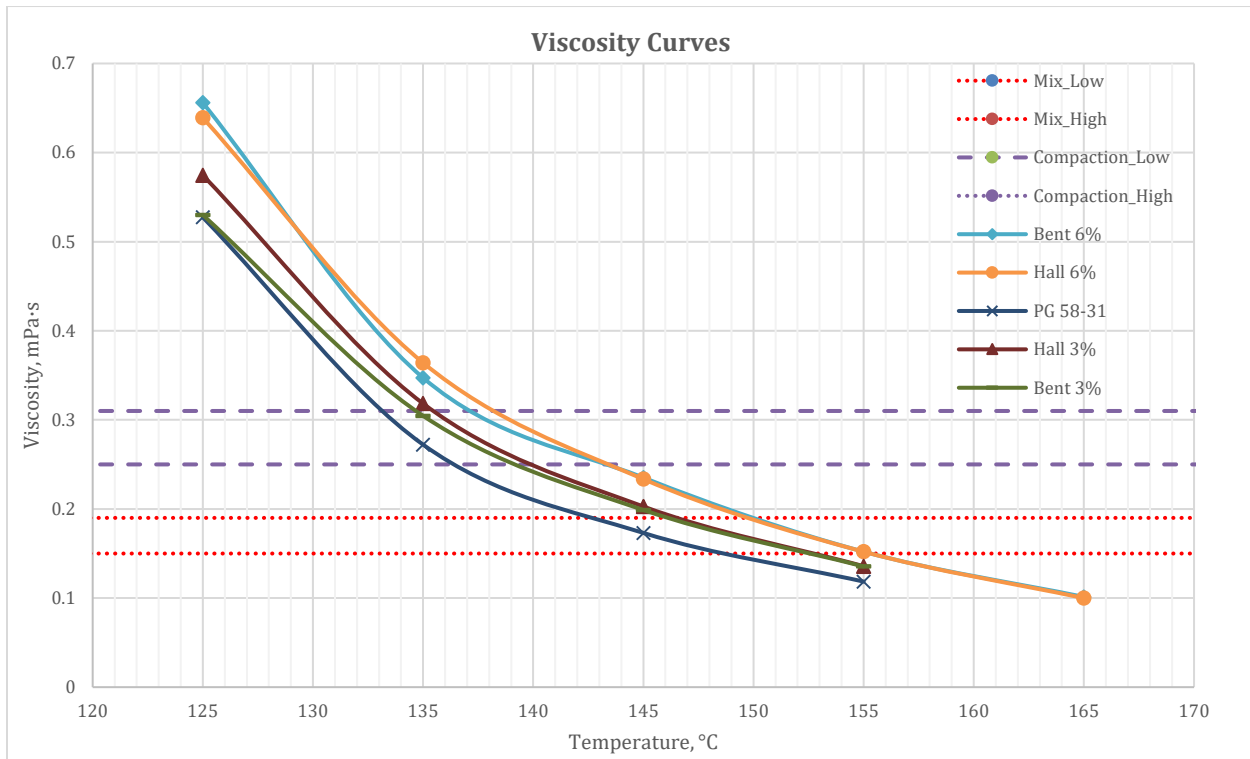


Figure 7: Viscosity Curves for PG 58-31 and four Nano-modified binders (3% and 6%-Halloysite, and 3% and 6%-Bentonite)

### Rutting Test

A Hamburg Wheel Tracker (HWT) was used to evaluate the rutting potential of the HMA samples. Based on AASHTO T324-16, this device tracks a  $705 \pm 4.5$  N, 47mm-wide steel wheel (at a frequency of  $52 \pm 2$  passes per minute and a maximum speed of 0.305m/s at midpoint) cyclically across a submerged HMA sample (cylindrical or slab), compacted to  $7.0 \pm 0.5\%$  or  $7.0 \pm 1.0\%$  (using a Superpave gyratory compactor or linear kneading compactor). This is continued for 20,000 passes or until a rut depth of 12mm is achieved, whichever is first, for a predefined temperature. A graph of rut depth vs. number of passes can provide valuable information about the rutting potential of asphalt concrete mixes, as well as their susceptibility to moisture damage (Aschenbrener, 1995).

### Sample Preparation

Using the same mix design and the mixing and compaction temperatures listed above, five sets of asphalt mixes, including unmodified binder, binder modified using 3% and 6% (by weight) bentonite nanoclay and binder modified using 3% and 6% of halloysite nanoclay, with air voids of 6-8% were prepared. The cooled samples were saw-cut along a secant line, such that when joined together in the high-density polyethylene molds, a gap of no greater than 7.5 mm was achieved between the molds (Figure 8).



Figure 8: HWTB Cylindrical specimens (saw-cut) in HDPE moulds before (left) and after (right) test

A total of five (5) types of samples were prepared and tested, and the results are tabulated below (Table 5). It was observed that neat asphalt (PG 58-31) showed a rut depth of 11.6 mm at 20,000 passes. Results from the halloysite- and bentonite-modified asphalt concrete specimens resulted in significant reductions of rut depth after 20,000 passes – approximately 30% reduction in rut depth for the 3% bentonite and halloysite and approximately 80% reduction in rut depth for the 6% bentonite and halloysite. Comparison of the two nanoclays, bentonite and halloysite, show a similar effect in terms of rutting resistance on the asphalt binder.

A comparison of the increase in the number of passes at the stripping inflection points for the nanoclay-modified samples and the neat binder samples shows that the addition of 3% halloysite and bentonite increased the number of passes by 80% and 55%, respectively; while the addition of 6% halloysite and bentonite increased the number of passes by 96% and 92%, respectively. These results indicate a significant improvement in the resistance of modified mixes to moisture damage with the addition of nanoclay to the binder.

**Table 5: HWTB Results (Mechanical Properties)**

S/No	Sample ID	Description	Test Temperature (°C)	Post Compaction Consolidation (mm)	Stripping Inflection Point (# of Passes/mm)	Rut Depth (mm)
1	A & B	PG 58-31	45	1.74	9179 / 3.86	11.60
2	A & B	PG 58-31 + Hall 3%	45	1.32	16529 / 4.69	7.83
3	A & B	PG 58-31 + Hall 6%	45	0.67	18022 / 2.12	2.29
4	A & B	PG 58-31 + Bent 3%	45	1.43	14260 / 3.95	7.84
5	A & B	PG 58-31 + Bent 6%	45	0.89	17693 / 2.97	3.21

## Indirect Tensile (IDT) Creep and Strength Test

The indirect tensile creep and strength tests were developed to evaluate the resistance of hot mix asphalt (HMA) to thermal cracking, and these tests have become the most promising method for predicting the low-temperature performance of asphalt concrete mixtures (Lytton, et al., 1993), (Christensen & Bonaquist, 2004). Creep compliance is defined as the rate at which the strain increases for a constant application of stress, that is, the time-dependent strain per unit stress, while indirect tensile strength gives the strength of HMA when subjected to tension.

To compare the low-temperature properties of samples modified with 6% nanoclay, specimens were prepared for each of the modified and unmodified binder types. All specimens were conditioned and tested using an IPC Global Universal Testing Machine (UTM-100) in accordance with AASHTO T322-07. Specimen deformations were measured using horizontal and vertical linear variable differential transducers (LVDTs) mounted on brass gauge points with a gauge length of 25 mm on each face of the specimen. Each specimen was loaded to a target creep load of 1 kN for 100 seconds, after which the strength test was conducted at a loading rate of 12.5 mm/min. The creep compliance [D(t)], tensile strength and fracture energy were calculated for each asphalt mix as explained below.

### Creep Compliance

Creep compliance was calculated as a function of horizontal and vertical deformation, gauge length over which the deformation is measured, dimensions of the test specimen, and magnitude of the static load, and is tabulated (Table 6) below. It is given by the formula:

$$D(t) = \frac{\Delta X_{tm,t} \times D_{avg} \times b_{avg}}{P_{avg} \times GL} \times C_{cmpl}$$

where:

D(t) = creep compliance at time t (kPa)<sup>-1</sup>

GL = gauge length (m)

D<sub>avg</sub> = average diameter of all specimens (m)

b<sub>avg</sub> = average thickness of all specimens (m)

P<sub>avg</sub> = average creep load (kN)

X<sub>tm,t</sub> = trimmed mean of the normalized, horizontal deformations of all specimen faces at time t (m)

The parameter C<sub>cmpl</sub> is a correction factor and is given by

$$C_{cmpl} = \text{correction factor} = 0.6354 \times \left(\frac{X}{Y}\right)^{-1} - 0.332$$

where:

$\frac{X}{Y}$  = absolute value of the ratio of the normalized, trimmed mean of horizontal deformation to the normalized, trimmed mean of vertical deformation at a time corresponding to half the total creep test time (typically 50 seconds) for all specimen faces.

### Tensile Strength

Based on the recommendation of the NCHRP Report 530, the tensile strength,  $S_{t,n}$ , was calculated as a function of the maximum load and then “corrected” to its “true” tensile strength (Christensen & Ramon, 2004). The tensile strength is given by the formula below, and tabulated in (Table 6) below:

$$S_{t,n} = \frac{2 \times P_{f,n}}{\pi \times b_n \times D_n}$$

$$\text{Tensile strength} = (0.78 \times S_{t,n}) + 38 \quad (\text{for psi})$$

$$\text{Tensile strength} = (0.78 \times S_{t,n}) + 0.262 \quad (\text{for MPa})$$

where:

$S_{t,n}$  = “uncorrected” tensile strength of specimen, (MPa)

$P_{f,n}$  = maximum load observed for specimen, (MN)

$b_n$  = thickness of specimen, (m)

$D_n$  = diameter of specimen, (m)

### Fracture Energy

An object’s resistance to crack growth, or toughness, is dependent on the energy absorbed as the crack advances. This energy, called the fracture energy, is associated with plastic flow and concentrated at the crack tip, a plastic zone where the material’s yield stress is present (Roylance, 2001). The fracture energy provides an indication of the propagation of cracks within asphalt pavement at low service temperatures. In this study, it was determined by calculating the area under the curve of the IDT tensile strength test using the trapezoidal method and dividing by the crack cross-section (ASTM D8225-19).

Table 6 summarizes the results of the IDT test for neat asphalt binder (PG 58-31) and the four nanoclay-modified samples (3% and 6% halloysite by weight and 3% and 6% bentonite by weight). Based on the results shown in the table, 6% bentonite and halloysite added to the base binder slightly reduced the tensile strength of the mix by approximately 1% and 3%, respectively, but increased the fracture energy by 20% and 2%, respectively. The table also shows that there is no significant effect on the creep compliance for 3% nanoclay in the base binder; however, the addition of 6% nanoclay causes a 12% to 69% reduction in the creep compliance when compared to the control mix.

**Table 6: Summary of IDT Test Results**

Parameters	PG 58-31	3% Bentonite-modified	6% Bentonite-modified	3% Halloysite-modified	6% Halloysite-modified
Creep compliance [D(t)], 1/GPa (-20°C)	0.0032	0.0032	0.0010	0.0035	0.0028
Poisson Ratio (-20°C)	0.054	0.167	0.239	0.070	0.210
Tensile strength ( $S_{t,n}$ ), MPa (-10°C)	3.72	3.73	3.67	4.15	3.62
Fracture Energy, kJ/m <sup>2</sup> (-10°C)	4.057	4.994	4.873	4.574	4.166

## CONCLUSIONS AND FUTURE STEPS

- Dynamic Shear Rheometer (DSR) results show that the modification of PG 58-31 with nanomaterials (hydrophilic bentonite nanoclay and halloysite nanoclay) results in an increase in the complex modulus (or stiffness) of the matrix, as well as an increase in the binder's resistance to rutting. The increase in stiffness is proportional to the concentration of the nanoclay.
- Rotational viscometer (RV) measurements confirmed this increase in stiffness and showed that the addition of nanoclay increased the viscosity of the modified binder and, consequently, the mixing and compaction temperatures.
- Permanent deformation test results using a Hamburg Wheel Tracker showed that the addition of either nanoclay significantly improved both the rutting resistance and moisture sensitivity of the modified mixes.
- HMA produced with a 3% nanoclay-modified binder provides a significant improvement in performance at low service temperatures. Moreover, although the 6%-nanoclay modification resulted in a slight reduction of the tensile strength of the mix, once a crack was initiated, its propagation seemed to be slower than that for HMA produced with the neat binder.
- The rheology of the asphalt binder and its nanoclay-modified equivalents provides a useful indication of the expected performance of the HMA produced at high, intermediate and low temperatures

To understand the mechanical properties of modified asphalt mixes at low temperatures, the next step for this research will be to perform rheological tests on nanoclay-modified binders at low temperatures, using a bending beam rheometer. Also, research will continue with conducting IDT tests at 0°C, as well as dynamic modulus testing.

## ACKNOWLEDGMENTS

The authors would like to acknowledge Husky Energy and Lafarge for providing the material for the research.

## REFERENCES

- AASHTO. (2010). *AASHTO T 315-10: Standard Method of Test for Determining the Rheological Properties of Asphalt Binder Using a Dynamic Shear Rheometer (DSR)*. (American Association of State Highway and Transportation Officials).
- Ajour, A. M. (1981). Several projects, several types of surfaces. *Bulletin of LCPA*, 113, 9-21.
- Alberta Transportation. (2010). *Standard Specifications for Highway Construction*. Edmonton, Alberta, Canada: Alberta Transportation.
- Aschenbrener, T. (1995). Evaluation of Hamburg Wheel-Tracking Device to Predict Moisture Damage in Hot Mix-Asphalt. *Transportation Research Record*, 1492, 193-201.
- Christensen, D. W., & Bonaquist, R. F. (2004). *Evaluation of indirect tensile test (IDT) procedures for low-temperature performance of hot mix asphalt*. Transportation Research Board.

- Christensen, D. W., & Ramon, F. B. (2004). *Evaluation of indirect tensile test (IDT) procedures for low-temperature performance of hot mix asphalt. Vol. 530* (Vol. 530). Washington D.C., United States of America: Transportation Research Board.
- Deepa, P., Laad, M., Sangita, & Singh, R. (2019, March 15). An overview of use of nanoadditives in enhancing the properties of pavement construction binder bitumen. *World Journal of Engineering*. doi:10.1108/WJE-04-2018-0136
- Federal Highway Authority/National Highway Institute. (2000). *Superpave Fundamentals Reference Manual*. National Highway Institute. Retrieved from <https://idot.illinois.gov/Assets/uploads/files/Transportation-System/Manuals-Guides->
- Ghile, D. (2006). *Effects of nanoclay modification on rheology of bitumen and on performance of asphalt mixtures*. Delft, The Netherlands: Delft University of Technology.
- Hossain, Z., Zaman, M., Hawa, T., & Saha, M. C. (2014). Evaluation of moisture susceptibility of nanoclay-modified asphalt binders through the surface science approach. *Journal of Materials in Civil Engineering*, 27(10), 04014261. doi:10.1016/j.measurement.2016.07.045
- Huang, W., Wang, D., He, P., Long, X., Tong, B., Tian, J., & Yu., P. (2019). Rheological Characteristics Evaluation of Bitumen Composites Containing Rock Asphalt and Diatomite. *Applied Sciences*, 9(5), 1023.
- Jahromi, S. G., & Khodaii, A. (2009). Effects of nanoclay on rheological properties of bitumen binder. *Construction and Building Materials*, 23(8), 2894-2904. doi:10.1016/j.conbuildmat.2009.02.027
- Leica Microsystems GmbH [DE]. (2018, September). Retrieved from <https://www.leica-microsystems.com/science-lab/brief-introduction-to-coating-technology-for-electron->
- Lytton, R. L., Uzan, J., Fernando, E. G., Roque, R., Hiltunen, D., & Stoffels, S. (1993). *Development and Validation of Performance Prediction Models and Specifications for Asphalt Binders and Paving Mixtures, Report SHRP-A-357*. Washington D.C.: Strategic Highway Research Program, National Research Council.
- Mallick, R. B., & El-Korchi, T. (2013). *Pavement engineering principles and practice. 2nd ed. CRC Press Taylor and Francis Group*. CRC Press Taylor and Francis Group.
- Marini J et al. (2014). Elaboration and properties of novel biobased nanocomposites with halloysite nanotubes and thermoplastic polyurethane from dimerized fatty acids. *Polymer*, 55(20), 5226-5234. Retrieved from <https://www.sigmaaldrich.com/catalog/product/aldrich/685445?lang=en&region=CA>
- Merck KGaA/Sigma-Aldrich. (2019). *Sigma-Aldrich*. Retrieved April 20, 2019, from <https://www.sigmaaldrich.com/catalog/product/aldrich/685445?lang=en&region=CA>

- Morgan, A. B. (2007). Polymer-Clay Nanocomposites: Design and Application of Multi-Functional Materials. *Material Matters: Chemistry Driving Performance*, 2(1), 21. Retrieved from [https://www.sigmaaldrich.com/content/dam/sigmaaldrich/docs/Aldrich/Brochure/al\\_material\\_matters\\_v2n1.pdf#page=20](https://www.sigmaaldrich.com/content/dam/sigmaaldrich/docs/Aldrich/Brochure/al_material_matters_v2n1.pdf#page=20)
- Roylance, D. (2001, June 14). Introduction to fracture mechanics. 1. Cambridge, Massachusetts: Massachusetts Institute of Technology.
- Sigma-Aldrich. (2018). 682659 ALDRICH: Nanoclay, hydrophilic bentonite - Specification Sheet (CAS Number: 1302-78-9; EC Number: 215-108-5; MDL Number: MFCD00132796). Retrieved from Sigma-Aldrich: <https://www.sigmaaldrich.com/catalog/product/aldrich/682659?lang=en&region=CA>
- Uzarowski, L., RIZVI, R., MAHER, M., & Rizzo, J. (2017). Pavement Quality—The Forgotten Subject. In . *TAC 2017: Investing in Transportation: Building Canada's Economy--2017 Conference and Exhibition of the Transportation Association of Canada*.
- Yao, H., You, Z., Li, L., Lee, C. H., Wingard, D., Yap, Y. K., & Goh, S. W. (2012). Rheological properties and chemical bonding of asphalt modified with nanosilica. *Journal of Materials in Civil Engineering*, 25(11), 1619-1630.
- Yue, Y., Abdelsalam, M., Luo, D., Khater, A., Musanyufu, J., & Chen, T. (2019, January). Evaluation of the Properties of Asphalt Mixes Modified with Diatomite and Lignin Fiber: A Review. *Materials*. 12(3), 400. doi:10.3390/ma12030400
- Zhu, W., Bartos, P., & Porro, A. (2004, November). Application of nanotechnology in construction; Summary of a state-of-the-art report. *Materials and structures*, 37(9), 649-658.